IEEE Access
Multidisciplinary | Rapid Review | Open Access Journal

Received July 21, 2021, accepted July 30, 2021, date of publication August 11, 2021, date of current version August 19, 2021.

Digital Object Identifier 10.1109/ACCESS.2021.3104098

Power Budgeting of LEO Satellites: An Electrical Power System Design for 5G Missions

ALI JIHAD ALI[1], (Graduate Student Member, IEEE), MOHSEN KHALILY[1], (Senior Member, IEEE), ATA SATTARZADEH[1], AHMED MASSOUD[2], (Senior Member, IEEE), MAZEN O. HASNA[2], (Senior Member, IEEE), TAMER KHATTAB[2], (Senior Member, IEEE), OKAN YURDUSEVEN[3], (Senior Member, IEEE), AND RAHIM TAFAZOLLI[1], (Senior Member, IEEE)

[1]Institute for Communication Systems (ICS), Home of 5G and 6G Innovation Centres, University of Surrey, Guildford GU2 7XH, U.K.
[2]Department of Electrical Engineering, Qatar University, Doha, Qatar
[3]Institute of Electronics, Communications & Information Technology, Queen's University Belfast, Belfast BT7 1NN, U.K.

Corresponding author: Ali Jihad Ali (ali.ali@surrey.ac.uk)

The work of Okan Yurduseven was supported by the Research Grant from the Leverhulme Trust through the Research Leadership under Award RL-2019-019.

ABSTRACT Although Geostationary-Equatorial-Orbit (GEO) satellites have achieved significant success in conducting space missions, they cannot meet the 5G latency requirements due to the far distance from the earth surface. Therefore, Low-Earth-Orbit (LEO) satellites arise as a potential solution for the latency problem. Nevertheless, integrating the 5G terrestrial networks with LEO satellites puts an increased burden on the satellites' limited budget, which stems from their miniature sizes, restricted weights, and the small available surface for solar harvesting in the presence of additional required equipment. This paper aims to design the Electrical Power System (EPS) for 5G LEO satellites and investigate altitudes that meet the latency and capacity requirements of 5G applications. In this regard, accurate solar irradiance determination for the nadir-orientation scenario, Multi-Junction (MJ) solar cells modeling, backup batteries type and number, and designing highly-efficient converters are addressed. Accordingly, the power budgeting of the 5G LEO satellite can be achieved based on defining the maximum generated power and determining the satellite's subsystem power requirements for 5G missions. In the sequel, the measured and simulated values of the electrical V-I characteristics of an MJ solar panel are compared to validate the model by using a Clyde Space solar panel that reaches a maximum power generation of approximately 1 W at ($I_{MPP} = 0.426\ A$, $V_{MPP} = 2.35\ V$). Moreover, a synchronous boost converter circuit is designed based on commercial off-the-shelf elements.

INDEX TERMS 5G, CubeSat, electrical power system (EPS), low-earth-orbit (LEO) satellites, multi-junction (MJ) solar cells.

I. INTRODUCTION

The vicinity to the earth, low-cost, relatively low complexity, and off-the-shelf elements are unique merits for LEO satellites; which have motivated researchers to consider them for communication systems. The interest in developing these satellites is increasing by leaps and bounds, mainly to be integrated with 5G terrestrial networks due to their acceptable latency values for many 5G scenarios, compared to the GEO satellites' high latency figures. Several papers have proposed schemes that utilize the high-capacity of GEO satellites and the low latency of LEO satellites at the same time. By this we mean building communication systems that consist, for instance, of one or more GEO satellites and a constellation of LEO satellites for high data rate satellite communications [1].

Although the importance of deploying LEO satellites to support the terrestrial communication networks has been emphasized in literature [2], obtaining LEO satellites that are capable of providing the same quality of service (QoS) as that of the terrestrial network remains a big challenge. Higher-quality connections would require more complex subsystems with higher power consumption demand. The LEO

The associate editor coordinating the review of this manuscript and approving it for publication was Yougan Chen.

satellites' limited power resources motivated the authors of [3] to propose a power effective solution with a system comprised of GEO satellite and a constellation of LEO satellites. They suggested improving GEO satellite antennas' receiving capabilities instead of increasing the transmitted power of the LEO satellite antennas. This, in turn, would decrease the burden of both the power consumption and the volume of the LEO satellites. It is a reasonable solution to improve the signal that reaches the LEO satellite instead of utilizing bigger or more equipment. Nevertheless, the high number of antennas in the 5G mission, which are required on the LEO satellite to support connections between the constellation's satellites, between GEO satellites and LEO satellites, and between LEO satellites and the earth, contributes to increasing the consumed power from the Electrical Power System (EPS).

In this paper, the optimal EPS characteristics of one common type of LEO satellites (Cubesat) are investigated for the 5G mission. To this end, the CubeSat's subsystems are defined, so the satellite's energy requirements can be specified. Generally, CubeSats have three main segments: execution, functional, and scientific. The execution segment is related to the CubeSat propulsion and movement technologies. The scientific segment depends mainly on the mission tools and sensors, while the functional segment consists of the EPS, Communication Subsystem (COM), Attitude Determination and Control Subsystem (ADCS), and On-Board Computer (OBC) [4].

The remainder of the paper is organized as follows: Section II surveys the state-of-the-art relevant to our work and provides a list of our contributions. The on-orbit incident solar irradiance for the chosen 1U (10cm $\times$ 10cm $\times$ 10cm) CubeSat is discussed in section III. Section IV introduces the MJ solar cells modeling. Section V covers the backup storage systems (battery's type and number). Following that, section VI proposes a scheme for synchronous converters design. Numerical results are presented in section VII, and finally section VIII concludes the contents of the paper.

II. RELATED WORK

Previous studies have investigated the development of CubeSat subsystems and addressed different challenging design concerns. For example, the CubeSat's high-speed movement while scanning the Earth needs effective equipment to achieve the desired altitude control [5]. In other words, an effective ADCS subsystem should alleviate the angular variations to avoid all the unexpected space disturbances [6]. The stable movement of satellites, which are orbiting based on a particular orientation scenario, allows for easier and accurate determination of the received solar irradiance to the satellite's sides. Hence, the satellite orientation should be maintained as much as possible [7]. Other papers presented the power limitations of these satellites for the communication missions as in [8].

To determine the generated power for CubeSats, it is crucial to study the relationship between the received solar irradiance on the satellite's sides. Hence, orientation scenarios play a key role in defining the amount of solar irradiance. In the literature, only few papers highlighted the effect of the orientation scenarios on the CubeSat performance [9], [10]. For example, the authors of [9] did not present the mathematical concepts of their work, which is focused mainly on the design of the Solar Module Integrated Converters (SMIC). In [10], the main orientation scenarios were introduced, taking into account the satellite altitude and the orbital parameters to evaluate their performance. However, the authors concentrated primarily on batteries' characteristics with a brief discussion of the principal source of power for the satellite and for recharging its batteries, which is the satellite's solar cells. Although [11] focused on several important aspects related to the optimal connection for the EPS components, this work did not address the solar irradiance with the orientation scenario.

Based on the fact that the incident solar irradiance excites the solar cells to generate power, it is essential to identify an accurate model of high-efficient solar panels to estimate the satellite's generated power on orbit during all CubeSat's trajectory stages.

The solar cells' latest development has led to engaging materials different from silicon in the cell structure [12]. Consequently, higher conversion efficiencies were obtained by the Multi-Junction (MJ) solar cells [13]. Several materials were exploited to achieve MJ solar cells so that each material absorbs a specific range of the solar irradiance spectrum, resulting in more irradiance being converted into electrical power. A high conversion efficiency performance has been captured using MJ solar cells in [14] and [15] by mitigating the chromatic aberration. It is worth noting that Five-Junction solar cells have recorded the highest efficiencies among all PV technologies [16].

Different models were devised to define the MJ solar cell parameters in different environmental conditions [17]. In [18], the authors introduced a general review of the existing modeling approaches for the high concentration MJ solar cells in terms of the cell parameters, the received irradiance, and the temperature. On the other hand, comprehensive analytical solutions for the single-diode and two-diode equivalent circuits were employed for modeling the MJ panels [19]. While four methods for studying the MJ cell's behavior were compared in [20], three of them are analytical, and the fourth is an algorithm for the optimization of nonlinear problems. The analytical methods in [19] and [21] presented approaches used to predict the V-I characteristics to ensure getting accurate models for the studied cells. Nevertheless, the results show some differences between the analytical and experimental validation.

Several methods of MJ parameter extraction have been investigated in the literature, such as curve fitting, fill factor, experimental results, and data-sheet information [22], [23]. In [22], the MJ parameters are obtained by curve fitting the cell's experimental characteristics, considering the single-diode model, which leads to steady-state errors in the final

values. On the other hand, the authors of [24] assumed the values of the overall series and parallel resistances, respectively, without highlighting the computation formula. In [25], the resistances were calculated depending on the empirical experiments in comparison to [26] and [27], where resistances were obtained from the V-I characteristics. Other papers did not discuss the resistances of each junction layer as in [23].

In this paper, the CubeSat power budgeting is considered as a critical enabler to the success of a CubeSat constellation for the 5G mission. A combination of related issues may affect the power budgeting. For example, it is vital to achieve a balance between a broad coverage area of the satellite network while maintaining low latency values [28], but this may influence the period of power generation. Another aspect that should be considered is the increased power consumption due to the number of used antennas [29], [30]. By this we mean, designing the EPS would experience many difficulties that should be carefully investigated. They are related to the orbit altitude, the coverage area, CubeSats high-speed movement, limited generated power under the significantly constrained size and volume resources, and 5G latency requirements [31], [32].

This paper continues the work started by the authors in [4], where several CubeSats applications were addressed besides discussing the main orientation scenarios of CubeSats with a focus on the nadir orientation scenario. In this paper, the modelling, analysis, and measurements of the EPS system are presented. By this we mean, several solar cells are simulated and the simulation results of the available solar cell are validated. Also, a new scheme for designing the EPS converters is proposed to achieve a high conversion efficiency where the previous method is employed to design and fabricate a high-efficiency boost converter. As a result, the optimal budgeting for the satellite power to meet the mission's necessary power is reached with the presented work starting from the input (irradiance determination) to the EPS (solar cells, batteries, and converters) and ending with the output (feeding the 5G CubeSat subsystems with the needed power).

A. PAPER CONTRIBUTIONS

The main contribution in this paper, versus existing aforementioned literature, is to introduce a scheme for budgeting the power of the 5G CubeSat satellite, which can be summarized in the following points:

- Employing the algorithm, presented in [4], to determine the received solar irradiance on the CubeSat's sides for nadir orientation scenario in a simple way without considering the direct cosine matrix and Euler 321 sequences as in [10]. Taking into account the chosen height ranges that guarantee the desired latency.
- Introducing an accurate model for the MJ solar cells.
- Defining the type and number of batteries for the 5G mission based on the 5G mission power requirements.
- Introducing a new scheme for designing high-efficiency converters.
- Validating the solar cells and converter models through comparison between the simulation and the experimental results.
- Designing the EPS circuit and applying the perturb & observation algorithm to obtain the maximum power point for the converters.

III. OPTIMAL SATELLITE ORIENTATION SCENARIOS

CubeSat satellites could have several orientation scenarios while they rotate around the earth, such as Nadir-Orientation, Free-Orientation, and Sun-pointing [4]. The nadir orientation scenario was chosen for the following reasons:

1) It is the most suitable option for the 1U CubeSat. For example, in the Sun-Pointing scenario, only one face always receives the radiation compared with the case of four faces that receive power in the nadir orientation scenario.
2) The 5G mission needs stable and accurate pointing towards the gateways and the User Equipment (UE) simultaneously. Hence, the free orientation scenario cannot guarantee the needed stability of connections between them.

Therefore, the nadir orientation is the potential orientation scenario for a CubeSat based 5G missions since it is always pointing towards the earth's center, as shown in Fig. 1. In this scenario, three sides could obtain maximum power generation: Z, $-Z$, and $-X$. Besides, X is exposed to the power for a short period before the eclipse stage and after it. Moreover, the satellite's angular location could be determined based on the approach presented in [4], so the solar irradiance variations through the satellite's path can be computed.

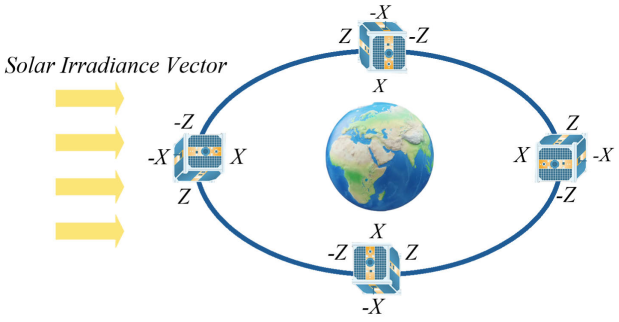

FIGURE 1. Nadir-pointing orientation scenarios.

This paper uses the approach proposed in [4] to calculate the incident solar irradiance on the sides of the satellite depending on the value of the angle β_i, which is the subtended angle between the satellite side and the direction of the solar irradiance, as depicted in Fig. 2. This figure exhibits two cases for β_i (the angle between the X-axis side and the solar irradiance direction). The first one is when it equals 90° (the maximum received radiation) and the second one is when the angle is 75°.

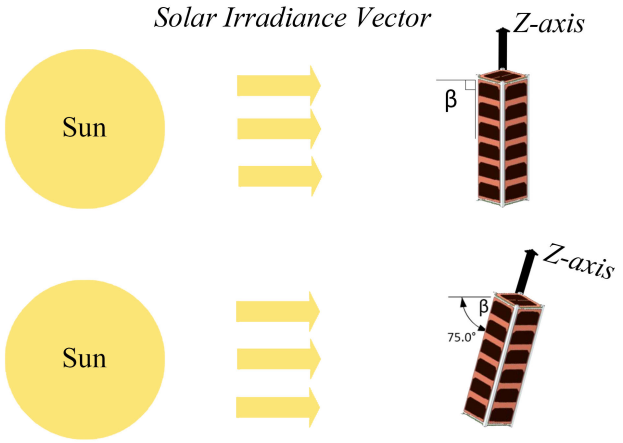

FIGURE 2. The proposed angle β (subtended between the satellite side and the solar irradiation vector).

The aggregate generated power in (2) can be represented by:

$$P_{in} = \sum_{s=1}^{6} P_{in_i} \tag{1}$$

where P_{in_i} is the amount of the generated power for each side [4].

Since CubeSats are proceeding along the eclipse zone regularly, the power generated by the solar cells is not adequate to maintain the flow of the satellite's operations. Moreover, in the illuminated zone, sometimes, the higher data rate demand or the increased number of users could lead to additional power consumption from the EPS. Consequently, equipping the EPS with batteries is fundamental to store enough energy for different payload conditions. Thus, the periods of illuminated and shadowed areas should be determined accurately, so batteries' capacity could be obtained as in [4], [33].

IV. MULTI-JUNCTION SOLAR CELLS

MJ solar cells have an increased conversion efficiency, for a given solar irradiance, owing to the usage of multiple p-n junctions made of several semiconductors (different energy bandgaps), as illustrated in Fig. 3. Consequently, each layer absorbs a different light spectrum, which boosts the produced power. Modeling is a vital tool to estimate the generated power by the solar cells. Accordingly, the CubeSat's generated power can be predicted before the launching process. For this reason, the following subsections will focus on modeling the Triple Junction (3J) solar cells.

Two main equivalent circuits are used for modeling 3J solar cells. The first one is the single-diode equivalent circuit model, and it uses five parameters: the diode reverse current, series and parallel resistors, generated currents, and thermal voltage, to study the cell characteristics. The second circuit model is the three-diodes circuit, where the circuit is represented using a more complex and precise model.

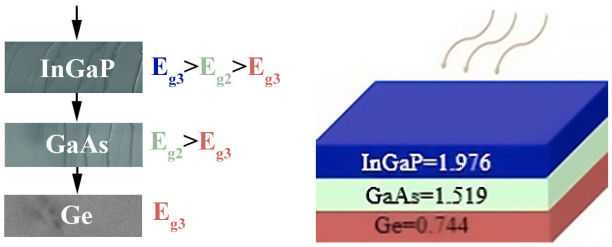

FIGURE 3. Triple-junction cells structure, where E_g is the energy band-gap of each substrate material.

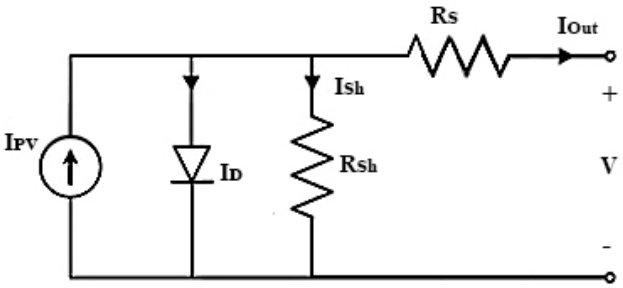

FIGURE 4. The single diode equivalent circuit.

A. APPROXIMATE MODEL WITH A SINGLE-DIODE CIRCUIT

In this approach, the 3J solar cell is approximated by the one diode equivalent circuit due to the easy calculations and the reduced number of employed parameters. The single-diode equivalent circuit is illustrated in Fig. 4 [25]. Here, the cell can be described as a source, a diode, and resistors, which present the power loss in connection points and through conductors.

B. DETAILED MODEL WITH THE THREE-DIODE CIRCUIT

This part presents the three diodes equivalent circuit for 3J solar cell modeling. As shown in Fig. 5, the equivalent circuit includes three-diode circuits connected to perform the layers of the three materials [20], [23], [24], [34]. The three circuits have a series connection that leads to the same current passing through them, and the output voltage is the sum of their voltages.

Using different materials means different saturation currents for each diode, which can be obtained using:

$$I_{Oi} = K_i . \left(\frac{T}{T_{Ref}}\right)^3 . \left(\exp\left(-\frac{q.E_{gi}}{n_i.K_B}.\left(\frac{1}{T}-\frac{1}{T_{Ref}}\right)\right)\right) \tag{2}$$

where in the three diodes calculations: $i \in [1, 3]$, the reverse saturation current of the diode is I_{Oi}, K_i represents the recombination current, T is the temperature, T_{Ref} is the reference temperature value, the charge of the electron is q, E_{gi} is the bandgap energy, n_i is the diode ideality factor, and K_B is Boltzmann constant.

The diode current is given as follows [23]:

$$I_{Di} = I_{Oi} . \left(\exp\left(\frac{q.V_{Di}}{n_i.K_B.T}\right) - 1\right) \tag{3}$$

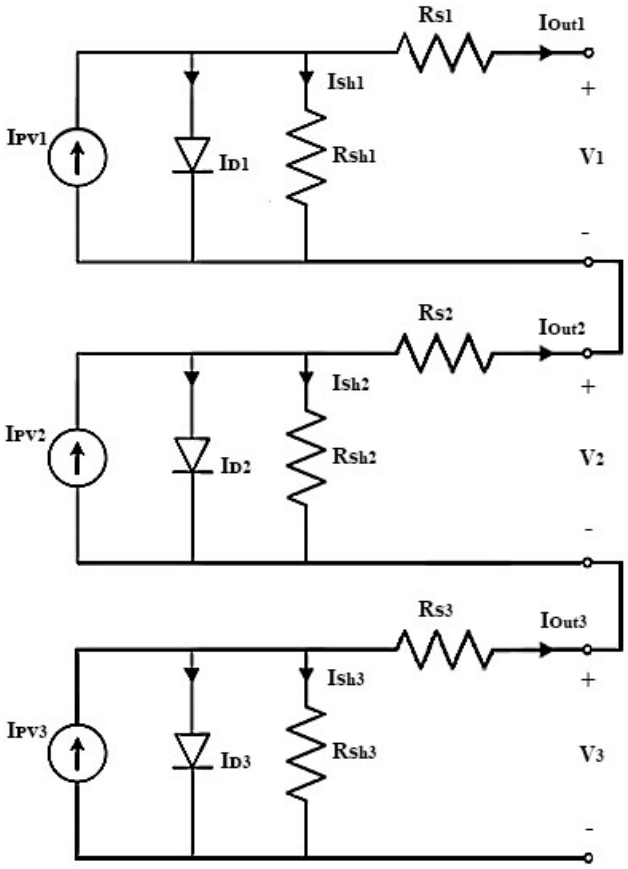

FIGURE 5. The three layers equivalent circuit of the triple-junction cell.

V_{Di} is the diode's voltage, and it is given as:

$$V_{Di} = V_i + I_{Out}.R_{Si} \tag{4}$$

where I_{Out} is the cell output current, and R_{Si} is the series resistance. Since it is difficult to obtain the values of each layer's series and parallel resistances, this paper relies on values reported in previous papers, which have conducted experimental calculations for the chosen cell resistances as in [22] and [25]. The layers voltage V_i is given as:

$$V_i = \frac{n_i.K_B.T}{q}.\ln\left[\frac{I_L - I_{Out}}{I_{Oi}} + 1\right] - I_{Out}.R_{Si} \tag{5}$$

On the other hand, the shunt current can be found as follows:

$$I_{Shunti} = \frac{V_i + I_{Out}.R_{Si}}{R_{Sh}} \tag{6}$$

where R_{Sh} is the parallel resistant.

The solar irradiance generated current is given by:

$$I_{PV} = \frac{S}{S_{ref}}\left(I_L + \frac{dI_{SC}}{dC}\left(T - T_{ref}\right)\right) \tag{7}$$

where S is the incident solar irradiance value, and S_{ref} is the Standard Test Conditions (STC) irradiance value 1353 W/m^2, whereas the current fraction represents the short-circuit current coefficient. Moreover, I_L represents the intensity of the solar irradiance at the location of the CubeSat and it can be expressed as follows:

$$I_L = I_{avg}.\left(1 - A.Cos\left(\theta_{Earth}\right)\right) \tag{8}$$

where I_{avg} is the intensity at the mean sun to earth distance W/m^2, A is the eccentricity of the orbit, and θ_{Earth} represents the angular position within the orbit.

The equivalent output current can be obtained as:

$$I_{Out} = I_{Outi} = I_{PVi} - I_{Di} - I_{Shunti} \tag{9}$$

Finally, the equivalent circuit voltage is:

$$V_{Out} = V_1 + V_2 + V_3 \tag{10}$$

V. THE ELECTRICAL POWER SYSTEM OF CUBESATS

In this paper, the amount of CubeSat satellites' generated power is determined for the 5G mission. It is assumed first that a trade-off between the coverage area and the satellite altitude is realized to record low latency values. It is known that the latency requirements for the 5G connection should not exceed 1 ms for the ultra-Reliable Low Latency Communication (uRLLC) services and 4 ms for the enhanced Mobile Broadband (eMBB) services. Consequently, to meet these requirements, the satellite altitude should range between 160 km above the equator (the latency would be around 1 ms) and 600 km above the equator (the latency would be 4 ms) [32]. However, deploying CubeSats at these altitudes is not practical for reasons concerned with the atmospheric drag and reduction in the life cycle of the satellite. Thus, CubeSats can be used in applications other than time-sensitive services such as the massive Machine Type Communications (mMTC) and 5G over satellite-like broadcast and multicast.

A. THE EPS DESIGN

The knowledge of the payload energy requirements is a principle factor before designing the EPS to guarantee a successful CubeSat mission. The solar cells, batteries, and converters (current/voltage adjusting circuits) are the backbone of the satellite's EPS. The only source of energy generation in satellites is the solar cells, whereas the storage system (backup batteries) supports the solar cells when the satellite in the shadowed zone or when the demanded energy is more than the generated one.

Several types of batteries are used for satellite missions, such as Lithium-Ion (Li-Ion), Nickel Cadmium (NiCd), and Nickel Metal Hybrid (Ni MH) [4]. Each type has its unique specifications, but the preferred type, for CubeSats missions, is the Li-Ion because it meets the constraints of mass and volume [35].

The required energy of the satellite's subsystems E_{tot} can be written as follows:

$$E_{tot} = \frac{E}{\eta} \tag{11}$$

where E represents the energy obtained from the solar cells, and η is the conversion stage efficiency. Therefore, we can

determine the accurate number of batteries to secure the needed amount of energy for CubeSat's subsystems. The solar cells' harvested energy is given as:

$$E_{sun} = \int_0^{T_{Sun-light}} P_{in}(t).dt \tag{12}$$

where $T_{Sun-light}$ is the interval in which the CubeSat receives the solar irradiance, and P_{in} (t) is the instantaneous received power. Thus, the batteries' energy is the difference between the total subsystems' requirements and the energy generated by the solar cells. The batteries' energy can be expressed as:

$$E^r_{batt} \geq \eta .(E_{sun} - \frac{T_{Sun-light}}{T_{orbit}} E_{tot}) \tag{13}$$

where E^r_{batt} is the energy required from satellite's batteries and T_{orbit} is the rotation period of the CubeSat around the Earth. As a result, one nominal battery energy can be described as follows [36]:

$$E_{batt} = \frac{(U_{\max} + U_{\min})}{2}.C \tag{14}$$

where the Li-Ion battery voltage limits are U_{max} and U_{min}, respectively, whereas C represents the battery capacity [Ah]. Hence, the needed number of batteries would be:

$$n = \left\lceil \frac{E^r_{batt}}{E_{batt}} \right\rceil \tag{15}$$

where $\lceil \cdot \rceil$ is the ceiling function.

VI. SYNCHRONOUS BUCK AND BOOST CONVERTERS

In this section, a new approach is implemented to obtain the optimal setup of the EPS converters' parameters. The regulation of voltages/currents is achieved using synchronous boost and buck converters. Hence, the number and type of converters are defined based on the CubeSat subsystems' voltage/current requirements. Fig. 6 displays the converters' design process, which starts with entering the output's desired efficiency, the frequency range, voltage/current ripples, and voltage/current margins. Then the duty cycle range is computed depending on the inserted parameters. Following that, the maximum values of inductance L and capacitance C are determined. After that, the designed converter efficiency is calculated based on the obtained parameters.

A. THE CONVERTER POWER LOSSES

The following power loss formulas were used to ensure obtaining the desired efficiency of converters. Based on the above-mentioned scheme, the power loss calculations are implemented continuously until reaching the converter's parameters, which guarantee minimum power losses.

1) CONDUCTION POWER LOSSES

The power dissipation of the converter components, such as inductor and capacitor resistances, leads to power losses, which can be expressed as follows [39]:

$$P_{cond} = P_{q1} + P_{q2} + P_{wr} + P_{esr} \tag{16}$$

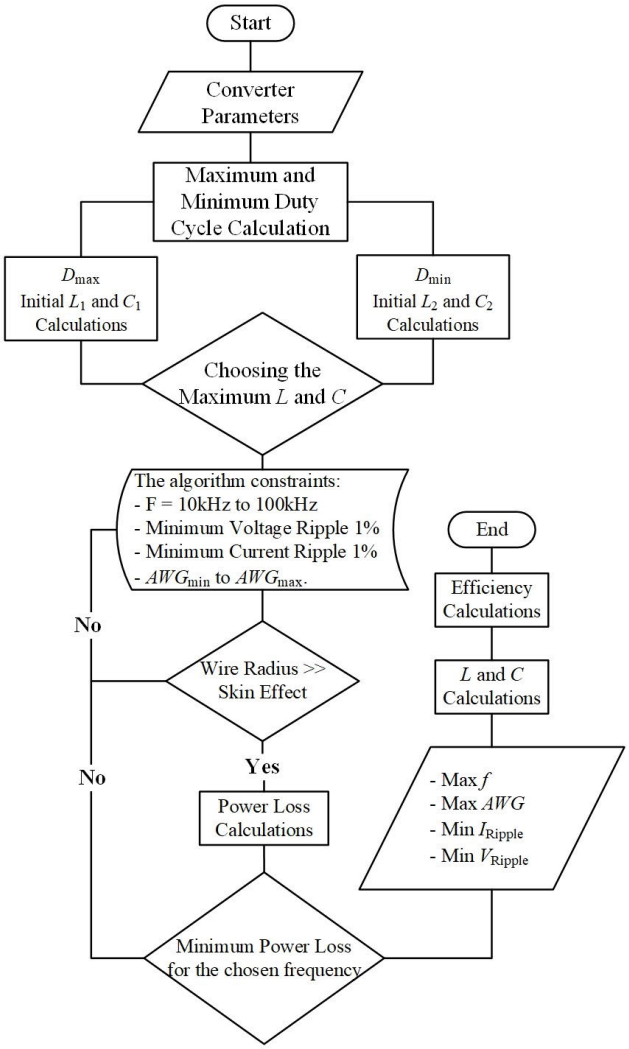

FIGURE 6. A flow chart for designing the EPS converters.

where P_{q1} and P_{q2} represent conduction losses due to the drain-source resistance R_{DS} for the case of using two instead of one MOSFET transistors and a single diode.

$$P_{q1} = I_{eff\,(max)}{}^2.R_{DS}.D \tag{17}$$

$$P_{q2} = I_{eff\,(max)}{}^2.R_{DS}.(1 - D) \tag{18}$$

where $I_{eff\,(max)}$ represents the maximum current, and D is the duty cycle. On the other hand, capacitor and inductor resistance losses (P_{esr} and P_{wr} respectively), are neglected for switching frequencies under 500 kHz.

2) SWITCHING POWER LOSSES

Each switching transition produces a power loss. Therefore, the total switching power loss is related to the switching frequency, and it can be obtained using:

$$P_{sw} = P_{turn} + P_{over} + P_{qrr} + P_{gate} \tag{19}$$

where P_{turn} represents the power loss of each switching cycle, and it can be calculated by:

$$P_{turn} = \frac{2}{3}.\left(CossL + CossH\right).V_{min}^{2}.f \tag{20}$$

where $CossH$ and $CossL$ are capacitances of transistors $TR1$ and $TR2$, respectively, whereas V_{min} is the minimum voltage value. The change in the transition state between switches generates power loss, which can be written as:

$$P_{over} = 0.5.I_{eff\,(max)}.t_f.f \tag{21}$$

where t_f is the falling time from on to off state.

The power loss due to the reverse recovery current can be expressed as:

$$P_{qrr} = Q_{rr}.V_o.f \tag{22}$$

where the reverse recovery charge is Q_{rr}.

Additional power loss could be caused by charging the gate-source capacitance C_{gs} of MOSFET transistors, which consumes power that could be computed by:

$$P_{gate} = Q_g.V_{max}.f \tag{23}$$

where Q_g is the charge of the gate.

It is worth mentioning that, the number of converters in the EPS subsystem can be reduced since it is not possible to illuminate two opposite sides of the satellite at the same time, for example, Z and $-Z$. Nevertheless, protection circuits would be needed in this case.

VII. NUMERICAL RESULTS

A. THE EPS DESIGN

The proposed CubeSat mission is to provide 5G services for the areas covered by its course, which means that the payload would mainly be the communication subsystem. To accomplish the mission requirements, the CubeSat should have three antennas; the first is for the feeder link, the second is an off-set parabolic reflector antenna for users link, and the third antenna would be used to relay data among the satellites of the constellation. CubeSat's subsystems' power and energy consumptions are displayed in Table 1 [36].

As can be seen in Table 1, the needed power is 12 W and we know that the selected satellite is a 1U CubeSat. Therefore, the first step, after considering the convenient altitude and the suitable orientation scenario, is to choose the solar cells, including the available surface that can be covered with solar cells and consequently the number of solar cells. Hence, the generated power can be obtained and the number of required batteries could be selected. As a case study, the Clyde Space (CS102834) cell is studied for the proposed EPS where the area by which a single side of the 1U CubeSat can receive solar irradiance is $A = 80.51\ cm^2$, knowing that the solar irradiance reaches around $1353\ W/m^2$. The maximum generated power is calculated for a cell's efficiency of 28.35%, which is the efficiency of (CS102834) cells:

TABLE 1. Satellite's power and energy requirements.

System	Voltage [V]	Current [A]	Time [h]	Energy [W.h]	Power [W]
OBC	5	0.125	1.54	0.9625	0.625
ADCS	5	0.75	0.25	0.09375	0.375
COM	5	2.2	1.54	16.94	11
Total Power	-	-	-	17.996	12

$$P_{in} = 3.08 + 0 + 0 + 0 + 0 + 0 = 3.08\ W$$

Depending on the nadir orientation scenario, only a single side would enjoy the maximum generated power, as the solar irradiation ultimately faces this satellite's side. Consequently, there is insignificant sun radiation received on the other sides that could be neglected. Studying the Albedo and the earth irradiance effect on the CubeSat is beyond this paper's scope, particularly for the 5G mission. CubeSats would have low altitudes to fulfill the requirements of the 5G applications. As a result, the proceeding factors would not have significant implications on the satellite's mission.

The net generated power, for a single side, is given by [4]:

$$P_{in1} = 2.88\ W$$

As it is evident in Table 1, both OBC and COM work almost during all the orbit period, which is logical since the payload is the communication subsystem. Assuming a 90% converters' efficiency and from (11), the total energy needed by the satellite is:

$$E_{tot} = 19.995\ W.h$$

For a CubeSat at an altitude of 400 km, the illuminated stage period is 56.36 minutes whereas the shadowed stage period equals 36.04 minutes. As a result, the sun-light stage generated energy is computed as per (12):

$$E_{sun} = 2.705\ W.h$$

So, the energy required from Li-Ion batteries to compensate for the CubeSat needs, i.e. that which solar cells cannot cover, is:

$$E_{batt}^{r} = 17.29\ W.h$$

The characteristics of the selected Li-Ion 18650 battery are:

- Nominal Voltage: 3.7 V
- Typical Capacity 2600 mAh
- The voltage's marginal values 4.2 V and 3 V

Consequently, the storage battery energy is ascertained by (14) as:

$$E_{batt} = 9.36\ W.h$$

Thus, the number of desired batteries is given as:

$$n = \left\lceil \frac{17.29}{9.36} \right\rceil = \lceil 1.84 \rceil = 2$$

Typically, satellites are equipped with battery packs that involve two or four batteries, such as Clyde Space and GOM Space products.

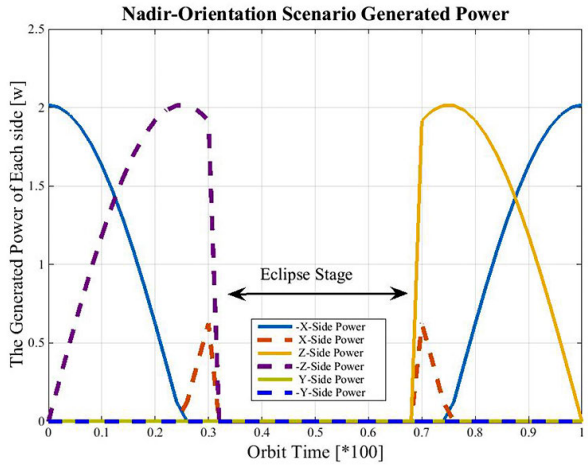

FIGURE 7. Satellite sides power variations.

TABLE 2. The InGaP/GaAs/Ge cells parameters.

Material	$E_g(0)$	$\alpha \times 10^{-4}$	β	K
InGaP	1.976	7.5	372	$1.86 * 10^{-9}$
GaAs	1.519	5.85	204	$1.22 * 10^{-8}$
Ge	0.744	4.774	235	$10.5 * 10^{-6}$

B. THE INCIDENT SOLAR IRRADIANCE

After choosing the nadir orientation scenario, the generated power for each satellite side could be determined. Since the CubeSat is in a continuous movement around the earth, the gained irradiance decreases and increases based on the difference between each side angle and the solar irradiance direction [4]. Fig. 7 illustrates the variations in the CubeSat's generated power depending on the side's inclination angle β.

C. MODEL VERIFICATION

In a pursuit to evaluate the proposed model, five triple-junction solar cells were employed, which are manufactured by AzurSpace (3G30A), Clyde Space (CS102834), SpectroLab (XTJ), SolAero (ZTJ-Ω), and Emcore (ZTJ). The bandgap energy and the material parameters for the used cells are given in Table 2, which shows Varshini coefficients to calculate the bandgap and the reserve saturation currents for each diode of the InGaP/GaAs/Ge substrates [23], [34]. Parameters obtained from manufacturers are V_{MP}, V_{OC}, I_{SC}, T_{Ref}, the cell area, and the solar cell efficiency, whereas the other parameters such as I_{O1}, I_{O2}, I_{O3}, and I_{PV} can be calculated as per (2) and (7). Note that the diode ideality factor values are assumed depending on the available experimental values in literature, and on surveying other 3J products [27]. Table 3 compares the nominal parameters and the simulated ones. It is clear that the proposed model shows an excellent matching percentage between the simulated and nominal parameters, which proves the accuracy of the results.

Fig. 8 shows the V-I characteristics for different 3J solar cells, which are AzurSpace (3G30A), SolAero (ZTJ-Ω), Clyde Space (CS102834), SpectroLab (XTJ), and Emcore (ZTJ) under the STC conditions. The convergence between

TABLE 3. Nominal and simulated currents and voltages of 3J cells.

	Simulated Current A	Nominal Current A	Simulated Voltage V	Nominal Voltage V	Matching Percentage
3G30A	0.496	0.502	2.348	2.409	96.3%
ZTJ-Ω	0.456	0.458	2.37	2.43	97.10%
CS102834	0.436	0.426	2.304	2.35	99.66%
XTJ	0.454	0.453	2.284	2.34	97.82%
ZTJ	0.445	0.4389	2.366	2.41	99.53%

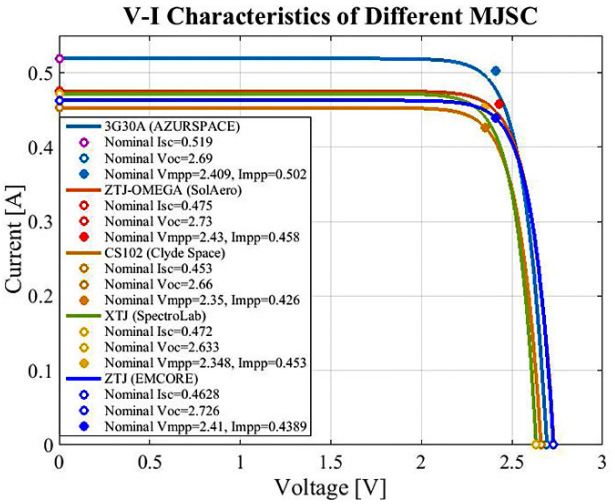

FIGURE 8. V-I characteristics for the chosen cells at 28°C. Colored circles represent data-sheet values.

the nominal values and the simulated ones is evident, knowing that the solid points represent the nominal maximum power points of each cell. It is clear that Clyde Space (CS102834) and Emcore (ZTJ) cells' performance is very close to the nominal maximum power points. It is worth mentioning here that the error in matching percentages is originated mainly from the errors in estimating the values of series and parallel resistances. Obtaining resistances from experimental results is the best way to ensure getting accurate values. However, this paper relies on previous papers in which experiments were conducted on 3J solar cells.

Fig. 9 illustrates V-P characteristics for the chosen cells under the STC conditions. Both the V-I and V-P characteristics demonstrate a high matching percentage between the simulated results and the nominal values of 3J solar cells that, in turn, validates the accuracy of the proposed model.

D. VERIFICATION OF THE PROPOSED MODEL USING CELL's MEASUREMENTS

The experiment was conducted on one of the body cells (CS102834) of the Qatar University (QU) CubeSat, produced by Clyde Space. Fig. 10 demonstrates the experiment instruments, which are:

1) Hydrogen light bulb.
2) The 3J cells.
3) Pyranometer sensor (Apogee SP-110), to measure the artificial irradiance on the panel.

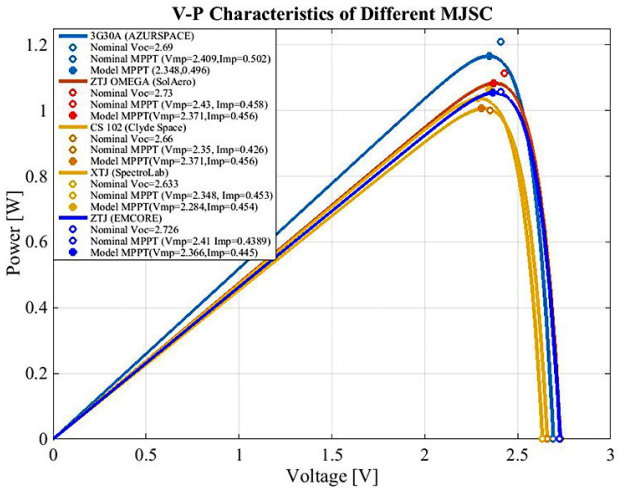

FIGURE 9. V-P characteristics of the chosen cells at 28° C. Colored circles represent the data-sheet values.

TABLE 4. The model verification.

Model	Nominal P_{max}	Simulated P_{max}	Percentage
[13]	-	-	95%
[24]	0.498	0.488	97.99%
[26]	-	-	96%
[38] D1	-	61.37	98.77%
[38] D2	-	61.68	99.1%
The Proposed Model	1.0045	1.0011	99.66%

TABLE 5. A comparison between converters efficiencies.

	Model	Average efficiency	Maximum power	Power converter
GOM Space	P31 U	95%	1-30 W	Boost
CLYDE Space	3UA	95%	-	PCM
Nano Avionics	-	96%	175 W	-
Proposed (model)	-	95.73%	20 W	Boost
Proposed (COTS elements)	-	92%	20 W	Boost

4) Three lists of resistances as the load.
5) Multimeters.

The experiment has been implemented under different irradiance and thermal conditions. Fig. 11 shows the comparison between the measured and the simulated characteristics of the cell under a temperature of $90°C$ and irradiance of $800\ W/m^2$. It is worth mentioning that there are two series-connected panels on each side, which is called 2S1P (two series on each parallel branch). Table 4 compares the accuracy percentage reached between the proposed model and other models addressed in the literature.

E. THE CONVERTER VERIFICATION

The scheme introduced previously for designing converters is utilized for designing a boost converter. Table 5 compares the achieved efficiency values for several manufactured converters and the converter proposed in this paper [39], [40]. The purpose of this comparison is to prove that the introduced scheme could produce viable and practical solutions. Fig. 12 shows the synchronous boost converter

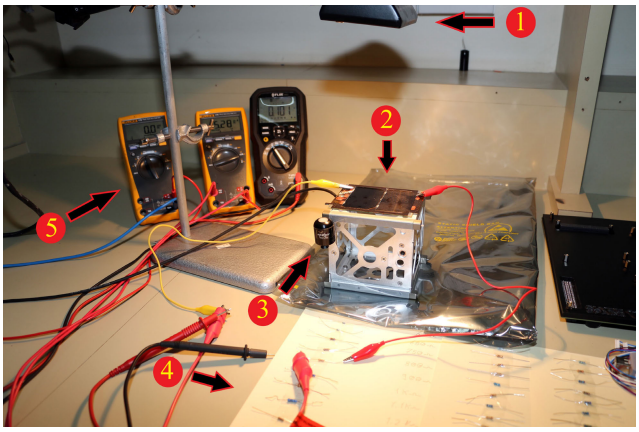

FIGURE 10. The 3J solar cell experimental testing.

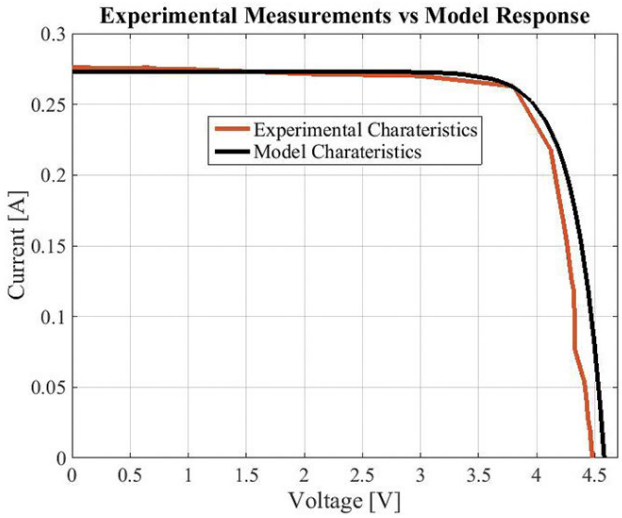

FIGURE 11. The CubeSat side panels characteristics based-on the experimental and model characteristics.

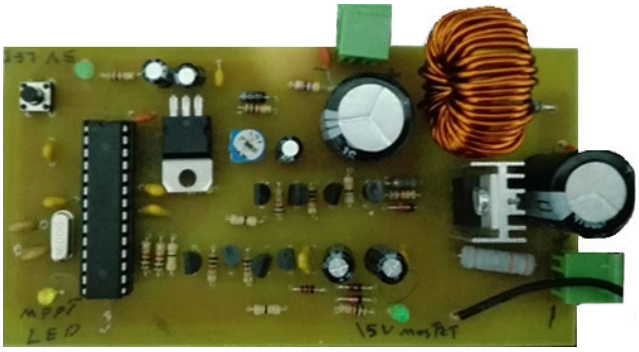

FIGURE 12. The designed synchronous boost converter.

circuit, which uses the Perturb and Observation algorithm $P\ \&\ O$ to track the maximum power point [11]. It should be noted that Atmeg 8 microcontroller and one MOSFET transistor IRF3205 were used to implement the $P\ \&\ O$ algorithm and to control the flow of currents effectively. Although the proposed converter efficiency seems lower than other converters' efficiency in Table 5, it achieves a very high efficiency since it uses COTS elements.

VIII. CONCLUSION

In this work, the basics of designing the EPS of CubeSats were addressed for the 5G mission. The power input of these satellites was covered by selecting the altitude, that considers the 5G latency, and the convenient orientation scenario, which meets the transmission consistency. Then the total amount of the received solar irradiance on the satellite's sides was determined. Next, a highly accurate model for several MJ panels, that harvest the solar irradiance, was introduced in an effort to predict the satellite's generated power, taking into account the efficiency of the used converters, which supply power to the satellite subsystems to guarantee the success of the mission. In addition, the solar irradiance of the satellite throughout its route, based on the nadir orientation scenario, was exhibited. Moreover, the 3J solar cells model was verified after doing measurements on the cells of QU CubeSat. Besides, the synchronous converter design was discussed and compared with other CubeSats' converters. To conclude, this paper addressed the input, the components of the EPS, and the output of the circuit that meets the latency and power requirements of a CubeSat, designed to join a constellation for a 5G mission.

The introduced work could be enhanced further by addressing the effect of the CubeSat's location concerning the sun and the earth in-depth, the former of which impacts the on-orbit power generation whereas the latter is concerned with the coverage area and the 5G load's power. Using more complex algorithms to track the maximum power-point would improve the generated power amount. Finally, addressing the link budget and discussing the subsystems' power requirements of the 5G payload would shed light on the obstructions of considering these satellites for the 5G missions and beyond.

ACKNOWLEDGMENT

This publication was made possible in part by the sponsorship agreement in support of research and collaboration by Ooredoo, Doha, Qatar. The statements made herein are solely the responsibility of the authors.

REFERENCES

[1] C. Wang, D. Bian, S. Shi, J. Xu, and G. Zhang, "A novel cognitive satellite network with GEO and LEO broadband systems in the downlink case," *IEEE Access*, vol. 6, pp. 25987–26000, 2018.

[2] I. Leyva-Mayorga, B. Soret, M. Röper, D. Wübben, B. Matthiesen, A. Dekorsy, and P. Popovski, "LEO small-satellite constellations for 5G and beyond-5G communications," 2019, *arXiv:1912.08110*. [Online]. Available: https://arxiv.org/abs/1912.08110

[3] L. Greda, B. Knüpfer, M. Heckler, J. S. Knogl, H. Bischl, and A. Drehe, "A satellite multibeam antenna for high-rate data relays," in *Proc. 32nd ESA Antenna Workshop Antennas Space Appl.*, 2010. [Online]. Available: https://www.researchgate.net/publication/225005134_A_Satellite_Multibeam_Antenna_for_High-Rate_Data_Relays

[4] A. Ali, A. Massoud, M. O. Hasna, T. Khattab, T. Jabban, and M. A. Nema, "Modeling of CubeSat orientation scenario and solar cells for internet of space provision," in *Proc. 9th Int. Conf. Recent Adv. Space Technol. (RAST)*, Istanbul, Turkey, Jun. 2019, pp. 541–546, doi: 10.1109/RAST.2019.8767869.

[5] P. E. Crouch, "Spacecraft attitude control and stabilization: Applications of geometric control theory to rigid body models," *IEEE Trans. Autom. Control*, vol. 29, no. 4, pp. 321–331, Apr. 1984.

[6] E. Martinez-de-Rioja, D. Martinez-de-Rioja, J. A. Encinar, A. Pino, B. Gonzalez-Valdes, Y. Rodriguez-Vaqueiro, M. Arias, and G. Toso, "Advanced multibeam antenna configurations based on reflectarrays: Providing multispot coverage with a smaller number of apertures for satellite communications in the K and Ka bands," *IEEE Antennas Propag. Mag.*, vol. 61, no. 5, pp. 77–86, Oct. 2019, doi: 10.1109/MAP.2019.2932311.

[7] K. Vega, D. Auslander, and D. Pankow, "Design and modeling of an active attitude control system for CubeSat class satellites," in *Proc. AIAA Modeling Simulation Technol. Conf.*, Aug. 2009, pp. 1–6, doi: 10.2514/6.2009-5812.

[8] O. Popescu, "Power budgets for cubesat radios to support ground communications and inter-satellite links," *IEEE Access*, vol. 5, pp. 12618–12625, Jun. 2017.

[9] J. Gonzalez-Llorente, A. A. Lidtke, K. Hatanaka, R. Kawauchi, and K.-I. Okuyama, "Solar module integrated converters as power generator in small spacecrafts: Design and verification approach," *Aerospace*, vol. 6, no. 5, p. 61, May 2019.

[10] S. Sanchez-Sanjuan, J. Gonzalez-Llorente, and R. Hurtado-Velasco, "Comparison of the incident solar energy and battery storage in a 3U CubeSat satellite for different orientation scenarios," *J. Aerosp. Technol. Manage.*, vol. 8, no. 1, pp. 91–102, Mar. 2016.

[11] I. T. Osman, "Design and implementation of EPS (electrical power system) of a CubeSat," M.S. thesis, Univ. Khartoum, Khartoum, Sudan, 2012.

[12] N. Fatemi, J. Lyons, and M. Eskenazi, "Qualification and production of emcore ZTJ solar panels for space missions," in *Proc. IEEE 39th Photovoltaic Spec. Conf. (PVSC)*, Tampa, FL, USA, Jun. 2013, pp. 2793–2796, doi: 10.1109/PVSC.2013.6745052.

[13] M. A. Mintairov, N. A. Kalyuzhnyy, V. V. Evstropov, V. M. Lantratov, S. A. Mintairov, M. Z. Shvarts, V. M. Andreev, and A. Luque, "The segmental approximation in multijunction solar cells," *IEEE J. Photovolt.*, vol. 5, no. 4, pp. 1229–1236, Jul. 2015.

[14] R. R. King, N. H. Karam, J. H. Ermer, N. Haddad, P. Colter, T. Isshiki, H. Yoon, H. L. Cotal, D. E. Joslin, D. D. Krut, R. Sudharsanan, K. Edmondson, B. T. Cavicchi, and D. R. Lillington, "Next-generation, high-efficiency III-V multijunction solar cells," in *Proc. Conf. Rec. 28th IEEE Photovoltaic Spec. Conf.*, Anchorage, AK, USA, Sep. 2000, pp. 998–1001.

[15] I. García, P. Espinet-González, I. Rey-Stolle, and C. Algora, "Analysis of chromatic aberration effects in triple-junction solar cells using advanced distributed models," *IEEE J. Photovolt.*, vol. 1, no. 2, pp. 219–224, Oct. 2011.

[16] D. H. Levi, M. A. Green, Y. Hishikawa, E. D. Dunlop, J. Hohl-Ebinger, and A. W. Y. Ho-Baillie, "Solar cell efficiency tables (version 51)," *Prog. Photovolt. Res. Appl.*, vol. 26, pp. 3–12, Dec. 2018.

[17] B. Padmanabhan, "Modelling of solar cells," M.S. thesis, Arizona State Univ., Tempe, AZ, USA, 2008.

[18] P. Rodrigo, E. F. Fernández, F. Almonacid, and P. J. Pérez-Higueras, "Models for the electrical characterization of high concentration photovoltaic cells and modules: A review," *Renew. Sustain. Energy Rev.*, vol. 26, pp. 752–760, Oct. 2013.

[19] D. S. H. Chan and J. C. H. Phang, "Analytical methods for the extraction of solar-cell single- and double-diode model parameters from I-V characteristics," *IEEE Trans. Electron Devices*, vol. 34, no. 2, pp. 286–293, Feb. 1987, doi: 10.1109/T-ED.1987.22920.

[20] L. E. P. Chenche, O. S. H. Mendoza, and E. P. B. Filho, "Comparison of four methods for parameter estimation of mono- and multi-junction photovoltaic devices using experimental data," *Renew. Sustain. Energy Rev.*, vol. 81, pp. 2823–2838, Jan. 2018.

[21] M. A. de Blas, J. L. Torres, E. Prieto, and A. García, "Selecting a suitable model for characterizing photovoltaic devices," *Renew. Energy*, vol. 25, no. 3, pp. 371–380, Mar. 2002.

[22] A. Ben Or and J. Appelbaum, "Dependence of multi-junction solar cells parameters on concentration and temperature," *Sol. Energy Mater. Sol. Cells*, vol. 130, pp. 234–240, Nov. 2014.

[23] H. Rezk and E.-S. Hasaneen, "A new MATLAB/Simulink model of triple-junction solar cell and MPPT based on artificial neural networks for photovoltaic energy systems," *Ain Shams Eng. J.*, vol. 6, no. 3, pp. 873–881, Sep. 2015.

[24] A. B. Hussain, A. S. Abdalla, A. S. Mukhtar, M. Elamin, R. Alammari, and A. Iqbal, "Modelling and simulation of single- and triple-junction solar cells using MATLAB/SIMULINK," *Int. J. Ambient Energy*, vol. 38, no. 6, pp. 613–621, Aug. 2017.

[25] S. Pindado and J. Cubas, "Simple mathematical approach to solar cell/panel behavior based on datasheet information," *Renew. Energy*, vol. 103, pp. 729–738, Apr. 2017.
[26] O. Shekoofa and J. Wang, "Multi-diode modeling of multi-junction solar cells," in *Proc. 23rd Iranian Conf. Electr. Eng.*, Tehran, Iran, May 2015, pp. 1164–1168.
[27] J. Cubas, S. Pindado, and F. Sorribes-Palmer, "Analytical calculation of photovoltaic systems maximum power point (MPP) based on the operation point," *Appl. Sci.*, vol. 7, no. 9, p. 870, Aug. 2017.
[28] L. A. Greda, A. Winterstein, A. Dreher, S. A. Figur, B. Schonlinner, V. Ziegler, M. Haubold, and M. W. Brueck, "A satellite multiple-beam antenna for high-rate data relays," *Prog. Electromagn. Res.*, vol. 149, pp. 133–145, 2014. [Online]. Available: https://www.jpier.org/PIER/pier.php?paper=14072502
[29] X. Liu, D. R. Jackson, J. Chen, J. Liu, P. W. Fink, G. Y. Lin, and N. Neveu, "Transparent and nontransparent microstrip antennas on a CubeSat: Novel low-profile antennas for CubeSats improve mission reliability," *IEEE Antennas Propag. Mag.*, vol. 59, no. 2, pp. 59–68, Apr. 2017.
[30] W. Liang, L. Raymond, M. Praglin, D. Biggs, F. Righetti, M. Cappelli, B. Holman, and J. R. Davila, "Low-mass RF power inverter for CubeSat applications using 3-D printed inductors," *IEEE J. Emerg. Sel. Topics Power Electron.*, vol. 5, no. 2, pp. 880–890, Jun. 2017.
[31] N. Saeed, A. Elzanaty, H. Almorad, H. Dahrouj, T. Y. Al-Naffouri, and M.-S. Alouini, "CubeSat communications: Recent advances and future challenges," *IEEE Commun. Surveys Tuts.*, vol. 22, no. 3, pp. 1839–1862, 3rd Quart., 2020, [Online]. Available: https://ieeexplore.ieee.org/document/9079470 and https://www.researchgate.net/publication/340881168_CubeSat_Communications_Recent_Advances_and_Future_Challenges, doi: 10.1109/COMST.2020.2990499.
[32] "Minimum requirements related to technical performance for IMT-2020 radio interface(s)," ITU-R, Standard Rep. M.2410, Nov. 2017. [Online]. Available: https://www.itu.int/pub/R-REP-M.2410-2017
[33] P. Gupta, *USUSAT II Micro-Satellite Power System (Theory, Design, and Testing)*. Logan, UT, USA: Utah State Univ., 2005, pp. 22–25.
[34] G. Segev, G. Mittelman, and A. Kribus, "Equivalent circuit models for triple-junction concentrator solar cells," *Sol. Energy Mater. Sol. Cells*, vol. 98, pp. 57–65, Mar. 2012.
[35] A. Ali, M. A. Nema, and T. Jabban, "Modeling and controlling of solar system for supplying CubeSat satellite," M.S. thesis, Dept. Elect. Power Syst. Eng., Aleppo Univ., Aleppo, Syria, 2019.
[36] R. D. Lazar, V. Bucelea, A. Loidl, L. Formanek, T. Chlubna, and S. B. Kjær, "Optimized design of power supply for CubeSat at Aalborg University," Aalborg Univ., Aalborg, Denmark, Tech. Rep. 139, 2002.
[37] J. Gonzalez-Llorente, D. Rodriguez-Duarte, S. Sanchez-Sanjuan, and A. Rambal-Vecino, "Improving the efficiency of 3U CubeSat EPS by selecting operating conditions for power converters," in *Proc. IEEE Aerosp. Conf.*, Mar. 2015, pp. 1–7.
[38] N. Das, H. Wongsodihardjo, and S. Islam, "Modeling of multi-junction photovoltaic cell using MATLAB/Simulink to improve the conversion efficiency," *Renew. Energy*, vol. 74, pp. 917–924, Feb. 2015, doi: 10.1016/j.renene.2014.09.017.
[39] *CubeSat Electrical Power System (EPS) of GOMSPACE*. Accessed: Nov. 12, 2020. [Online]. Available: https://gomspace.com/shop/subsystems/power/nanopower-p31u.aspx
[40] *CubeSat Electrical Power System (EPS) of NanoAvionics*. Accessed: Nov. 12, 2020. [Online]. Available: https://nanoavionics.com/cubesat-components/cubesat-electrical-power-system-eps/

ALI JIHAD ALI (Graduate Student Member, IEEE) received the B.Sc. degree in control engineering and automation (runner-up) and the M.Sc. degree (Hons.) in renewable energy and environmental engineering from Aleppo University (AU), Syria. He is currently pursuing the Ph.D. degree in information and communication systems program with the Institute for Communication Systems (ICS), Home of 5G and 6G Innovation Centres, University of Surrey, U.K. His research interests include the areas of LEO satellites power systems, 5G networks, reflectarrays antennas, and communication systems-based UAVs. From 2015 to 2020, he worked as a Research Assistant with Aleppo University. He worked as a Research Assistant with Qatar University in 2018.

MOHSEN KHALILY (Senior Member, IEEE) is currently a Lecturer in antenna and propagation with the Institute for Communication Systems (ICS), Home of 5G and 6G Innovation Centres, University of Surrey, U.K., where he was a Research Fellow of antennas and propagation, from December 2015 to March 2019. Prior to joining 5GIC, he was a Senior Lecturer with the Wireless Communication Centre (WCC), University Technology Malaysia (UTM).

He has published almost 100 academic articles in international peer-reviewed journals and conference proceedings. His research interests include surface electromagnetic, large intelligent surface, metasurfaces, dielectric resonator antennas, MIMO antennas, phased arrays, circularly polarized antennas for satellite application, hybrid beam-forming, leaky wave antennas, and mm-wave and terahertz antennas and propagation. He is a fellow of the U.K. Higher Education Academy. He is also a member of the IEEE Antennas and Propagation Society, the IEEE Communication Society, and the IEEE Microwave Theory and Techniques Society. He is an Associate Editor of the IEEE ACCESS.

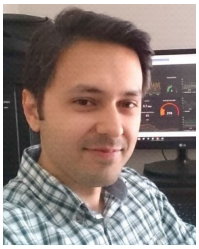

ATA SATTARZADEH received the B.Sc. degree in electrical engineering from the K.N.T University of Technology, the M.Sc. degree in telecommunications from IUST, and the Ph.D degree in telecommunications from the University of Tehran, Iran.

He is currently a Research Fellow with the 5G Innovation Centre, Institute for Communication Systems, University of Surrey. His research interests include 5G networks, satellite communication, and signal processing.

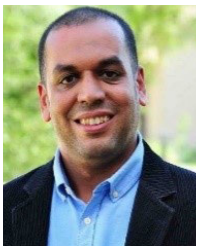

AHMED MASSOUD (Senior Member, IEEE) received the B.Sc. (Hons.) and M.Sc. degrees in electrical engineering from Alexandria University, Egypt, in 1997 and 2000, respectively, and the Ph.D. degree in electrical engineering from Heriot-Watt University, Edinburgh, U.K., in 2004.

He is currently the Associate Dean for Research and Graduate Studies and a Full Professor with the Department of Electrical Engineering, College of Engineering, Qatar University. He holds five U.S. patents. He has published more than 100 journal articles in the fields of power electronics, energy conversion, and power quality. His research interests include power electronics, energy conversion, renewable energy, and power quality.

MAZEN O. HASNA (Senior Member, IEEE) received the B.S. degree from Qatar University, Doha, Qatar, in 1994, the M.S. degree from the University of Southern California at Los Angeles, Los Angeles, CA, USA, in 1998, and the Ph.D. degree from the University of Minnesota Twin Cities, Minneapolis, MN, USA, in 2003, all in electrical engineering.

In 2003, he joined the Department of Electrical Engineering, Qatar University, where he is currently a Professor. From 2005 to 2017, he has served in several administrative capacities for Qatar University, including the EE Department Head, the College of Engineering Dean, the Vice President, and the Chief Academic Officer. His research interests include the general area of digital communication theory and its application to the performance evaluation of wireless communication systems over fading channels. His current specific research interests include cooperative communications, UAV-based networks, physical layer security, and FSO/RF hybrid networks. He appears in the 2015 highly cited researchers list of Clarivate Analytics. He is a Founding Member of the IEEE Qatar Section and served as its founding VP and currently serves on the joint management committee of Qatar Mobility Innovation Center.

TAMER KHATTAB (Senior Member, IEEE) received the B.Sc. and M.Sc. degrees in electronics and communications engineering from Cairo University, Giza, Egypt, and the Ph.D. degree in electrical and computer engineering from The University of British Columbia (UBC), Vancouver, BC, Canada, in 2007.

From 1994 to 1999, he was with IBM WTC, Giza, as a Development Team Member, and then as a Development Team Lead. From 2000 to 2003, he was with Nokia (formerly Alcatel Canada Inc.), Burnaby, BC, Canada, as a Senior Member of the technical staff. From 2006 to 2007, he was a Postdoctoral Fellow with The University of British Columbia, where he was involved in prototyping advanced Gbits/s wireless LAN baseband transceivers. He joined Qatar University (QU) in 2007, where he is currently a Professor of electrical engineering. He is also a Senior Member of the technical staff with Qatar Mobility Innovation Center (QMIC), a research and development center owned by QU and funded by Qatar Science and Technology Park (QSTP). In addition to more than 150 high-profile academic journal and conference publications, he has several published and pending patents. His research interests include physical layer security techniques, information-theoretic aspects of communication systems, radar and RF sensing techniques, and optical communication.

OKAN YURDUSEVEN (Senior Member, IEEE) received the B.Sc. and M.Sc. degrees in electrical engineering from Yildiz Technical University, Istanbul, Turkey, in 2009 and 2011, respectively, and the Ph.D. degree in electrical engineering from Northumbria University, Newcastle Upon Tyne, U.K., in 2014.

He is currently a Senior Lecturer (an Associate Professor) with the School of Electronics, Electrical Engineering and Computer Science, Queen's University Belfast, U.K. He is also an Adjunct Professor with Duke University, USA. From 2018 to 2019, he was a NASA Research Fellow at the Jet Propulsion Laboratory, California Institute of Technology, USA. From 2014 to 2018, he was a Postdoctoral Research Associate with the Department of Electrical and Computer Engineering, Duke University. He has been the Principal Investigator on research grants totaling in excess of £1.3 m in these fields. He has authored more than 130 peer-reviewed technical journals and conference papers. His research interests include microwave and mm-wave imaging, multiple-input-multiple-output (MIMO) radars, wireless power transfer, antennas and propagation, and metamaterials. He has served as a Technical Program Committee Member of SPIE Defense and Commercial Sensing conference, since 2020, and the Guest Editor in several journals, including IEEE Antennas and Wireless Propagation Letters, IEEE Open Journal of Antennas and Propagation, and *Remote Sensing* (MDPI).

He is a member of the European Association on Antennas and Propagation (EURAAP). In 2017, he received an Outstanding Postdoctoral Award from Duke University. He was a recipient of the NASA Postdoctoral Program Fellowship administrated by the Universities Space Research Association (USRA), in 2018. In 2019, in collaboration with the University of Limoges, France, he received the Alliance Hubert Curien Award funded by the British Council. In 2020, he was bestowed Leverhulme Trust Research Leadership Award. He has been served as a Technical Program Committee Member of SPIE Defense and Commercial Sensing conference, since 2020, and the Guest Editor in several journals, including IEEE Antennas and Wireless Propagation Letters, IEEE Open Journal of Antennas and Propagation, and *Remote Sensing* (MDPI). He serves as an Associate Editor of the IEEE Antennas and Wireless Propagation Letters.

RAHIM TAFAZOLLI (Senior Member, IEEE) has been a Professor of mobile and satellite communications, since April 2000. He has also been the Director of ICS, since January 2010, and the Founder and the Director of the 5G Innovation Centre, University of Surrey, U.K. He has more than 25 years of experience in digital communications research and teaching. He has authored or coauthored more than 500 research publications. He is a co-inventor of more than 30 granted patents, all in the field of digital communications. He is regularly invited to deliver keynote talks and distinguished lectures to international conferences and workshops.

In 2011, he was appointed as a fellow of the Wireless World Research Forum (WWRF) in recognition of his personal contributions to the wireless world and the heading one of Europe's leading research groups. He is regularly invited by many governments for advice on 5G Technologies. He was an Advisor to the Mayor of London with regard to the London Infrastructure Investment 2050 Plan, from May to June 2014. He has given many interviews to international media in the form of television, radio interviews, and articles in the international press.